Connection between the Impregnation of Glass Multi-Filament Yarns and their Pull-out Behaviour

Bruno Fiorio[1], Hana Aljewifi[2], Jean-Louis Gallias[3]

Summary: This experimental study focuses on the links that exist between the mechanical pull-out behaviour of multi-filament yarns embedded in concrete and the impregnation of the yarn by the concrete. To this aim, 5 glass yarns have been embedded in concrete (AR and E glass yarns from assembled or direct roving). A pre-treatment was applied to the yarn before the casting, and was chosen in the following three: wetting, drying or pre-impregnation with a cement slurry. By this way, 15 yarn / pre-treatment combinations were obtained that generate 15 conditions of impregnation of the yarn by the cementitious matrix. In each case, the mechanical properties were determined from a classical pull-out test and the yarns impregnation properties were characterized by two dedicated tests: yarns porosity measurements and along yarn water flow measurements.

By studying the relationship between the mechanical behaviour and the physical properties of the impregnated yarns, it is shown that the pre- and post-peak behaviour are mainly connected to the flow rate measured during the water flow measurements, which suggest a specific influence of the connected pores parallel to the filaments and of the penetration depth of the matrix into the yarn. The post-peak and the residual behaviour are moreover linked to the yarn pore volume associated to the disorder induced in the filaments assembly by the penetration of the matrix. The overall result of this work is a contribution to the understanding of the relationship between the impregnation of the yarns and the pull-out behaviour.

[1] Ass. Prof., Université de Cergy-Pontoise, L2MGC
[2] PhD student, Université de Cergy-Pontoise, L2MGC
[3] Prof., Université de Cergy-Pontoise, L2MGC

1 Introduction

Glass fibre reinforced cement composite have been used for many nonstructural applications since the early 1970s. An important step in the development of this kind of reinforcement was the introduction of the first alkali-resistant (AR) glass fibre about four decades ago (JESSE [1]). As AR glass fibres have low sensitiveness to corrosion when used in concrete, the concrete cover can be reduced in order to minimize the thickness of the structural members. This reduction is particularly high in the case of textile reinforced concrete (TRC).

The properties, performances and applications of TRC have been described by many authors (see for instance BRAMESHUBER [2], HEGGER ET AL. [3], HANISCH ET AL. [4]). Current studies have confirmed that complex processes of interaction occur inside the composite between the yarns and the cementitious matrix, and inside the yarns between the filaments and the penetrating cement paste or between the filaments themselves (KONRAD ET AL. [5]). These interactions are largely influenced by the yarns impregnation (PELED ET AL. [6]), and govern the mechanical properties of the TRC.

This aspect is one of the difficulties encountered when developing mechanical models of the yarn / matrix interaction. The partial penetration of the cementitious matrix in the yarn generates schematically two types of filaments: sleeve filaments anchored in the matrix and core filaments that remain approximately un-anchored. (OHNO ET AL.[7], LANGLOIS [8]). Generally, models use global parameters to take into account the complexity of the impregnation. These parameters have to be determined by identification of experimental results and may be largely disconnected from the physical state of the impregnation (HAÜßLER-COMBE ET AL. [9], LANGLOIS [8]). A better understanding of the impregnation is needed to improve the link between the mechanical results of the models and the initial physical data. With this aim, an experimental study was conducted to examine the relationship between global physical parameters related to the yarn impregnation and parameters characteristic of the mechanical pull-out behaviour.

2 Manufacturing of concrete samples with embedded yarn

2.1 Yarns characteristics and preparation

Samples used in this study were made of a single yarn embedded in a cylinder of cementitious matrix (see ALJEWIFI ET AL. [10] for more details). The yarn was aligned along the cylinder axis and was pre-treated before casting.

Five different kinds of multi-filament yarns have been used (four of them are an assembly of bundles of filaments, the last one is a direct assembly of filaments). Table 1 gives the basic properties of these yarns. It should be noticed that the geometrical properties of the yarns are much more numerous than those given in table 1, due to the multi-scale assembly of the fila-

ments (number and aspect ratio of bundles, for instance, can vary from one yarn to the other). Moreover glass filaments were coated with a sizing which influenced the yarn processing but also the adhesion with the matrix. Sizing materials were a mix of polyhydroxy-phenols, silane, polymer emulsion and additives. The detailed compositions of the sizing are unknown due to the industrial protection imposed by manufacturers.

Before casting, one of the following three pre-treatments was applied to the yarn, to generate different kinds of impregnation for each type of yarn:

– Pre-wetting (W): yarn was saturated with water prior to the casting so that the inter-filament voids are filled with water, which strongly reduce the penetration of cement paste inside the yarn during casting. It should be noticed that in this case, capillarity forces induce agglomeration of the glass filaments. Consequently, the inter-filament distances were reduced compared to what is observed in the case of dry yarns.

– Drying (D): yarn was dried at room temperature before casting. Capillarity forces lead to penetration of water and cement particles in the yarn during casting. As the filaments act as a filter, penetration of cement particles into the yarn was generally limited.

– Cement pre-impregnation (PI): the yarn was manually saturated with a cement slurry before casting. Saturation was obtained by manual action on the yarn placed in a slurry batch. The composition of the slurry was identical to those of the cement paste of the matrix.

Table 1: Physical and mechanical characteristics of the multi-filaments yarns.

	SG1	SG2	SG3	OC1	OC2
Type of glass	AR	AR	AR	E	E
Type of roving	Assembled	Assembled	Assembled	Assembled	Direct
Filament diameter (μm)	14	14	14	12	17
Finesses (tex =g/km)	2450	2450	2500	2400	2400
Glass density (kg/m^3)	2680	2680	2680	2530	2530
Max.strength (N)	741.4	856.6	830.4	1116.3	900.5
Yarn stiffness (GPa)	56.5	44.9	45.5	54.8	55.9

2.2 Fine grained concrete design and sample elaboration

The pre-treated yarn was positioned along the axis of a cylindrical mould (34 mm diameter) in which the cementitious matrix was poured. The matrix was a fine grained concrete made from CEM 1 52.5 N cement (0.48 water on cement ratio; 1.4 sand on cement ratio with 0-1.25 mm sand; a superplasticizer was used with a dry extract dosage of 0.125 % of the cement mass).

The main properties of the matrix were as follow: 2.135 g/cm^3 density, 31.5 GPa Young's modulus, 55 MPa compressive strength. The fresh matrix was fluid, with no segregation of the sand aggregates.

Cylindrical samples were made with height, i.e. embedded length of the yarn in concrete, chosen in the following series: 1 cm, 3 cm, 5 cm, 10 cm, 15 cm and 25 cm. Samples were removed from mould 24 hours after casting. Water curing at room temperature (20°C) was then imposed during 28 days before testing.

2.3 Qualitative aspects of the yarn impregnation

The pre-treatment has a strong influence on the resulting impregnation of the yarn by the matrix. To characterize the impregnation for each case (one yarn and one given pre-treatment), scanning electron microscopy (SEM) observations of longitudinal sections of impregnated yarns have been made. Longitudinal sections were obtained by splitting the cylinder of fine grained concrete described in section 2.2 using a transverse compressive load. This method was chosen for its capability to give a view of all the yarn impregnation which is not the case with specific cross sections. It needs to take care of the disorganization of the yarn which is induced by the mechanical splitting but gives good results as far as information about micro-cracking is not needed.

Fig. 1 and Fig. 2 show examples of SEM observations respectively made for SG3 and OC2 yarns, for the three different pre-treatments of the yarn that have been used. These two yarns are representative of what is observed for the five yarns. ALJEWIFI ET AL. [10] give the full observations made for the five yarns.

The penetration of the cement paste appears as largely influenced by the pre-treatment. In the case of SG3 yarns (Fig. 1), the W pre-treatment gives the poorest impregnation, with large portions of filaments uncovered by the cementitious matrix in the center of the yarn. D pre-treatment shows evidences of deep penetration of the matrix inside the yarn, even if in some places filaments remain uncovered. PI pre-treatment gives a full impregnated yarn, with spread bundles separated by matrix.

In the case of the W pre-treatment, OC2 yarns (Fig. 2) shows parallel mainly non-impregnated filaments, with a thin layer of impregnated filaments. D pre-treatment gives a similar aspect, but with misalignment of the filaments and presence of hydrated products in some places inside the yarn. PI pre-treatment gives a full impregnation of the filaments. Compare to SG3, because of the specific structure of the OC2 yarn (direct roving), the filaments and the matrix are in this case very intimately mixed.

For W and D pre-treatments, other yarns (SG1, SG2 and OC1) show similar behaviour towards the impregnation. The main differences concern the impregnation in the case of the D pre-treatment, which appears as more dependent on the type of yarn than other pre-

treatments. This can be explained by the fact that, for the D pre-treatment, the penetration of the cement paste inside the yarn is mainly governed by the capillarity forces which are sensitive to the surface properties of the filaments (sizing) and to their geometry (diameter).

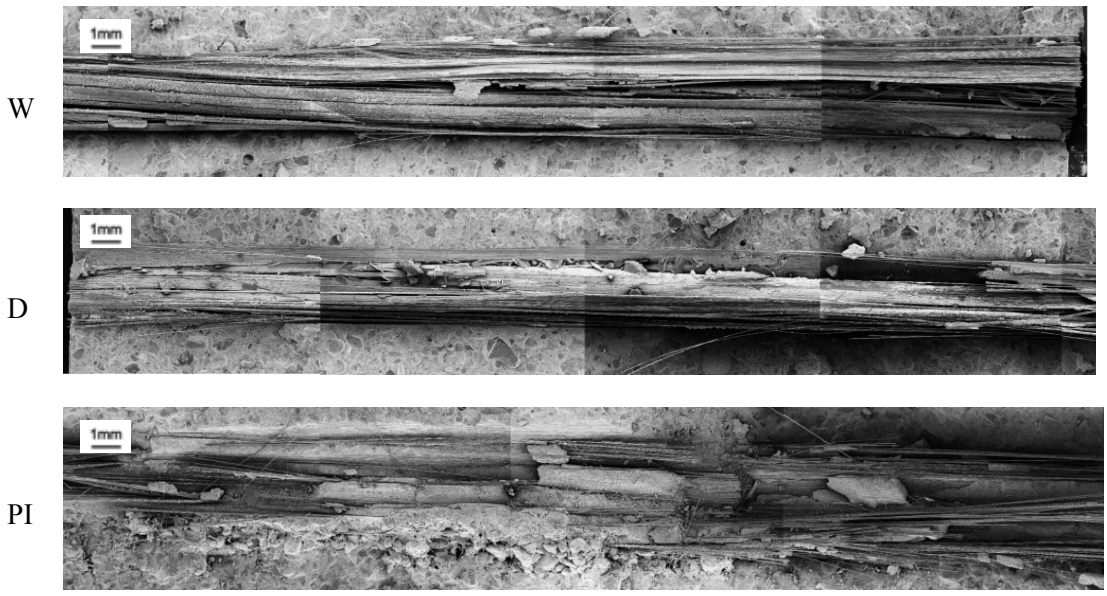

Fig. 1: SG3 yarn; longitudinal sections; W, D and PI pre-treatments.

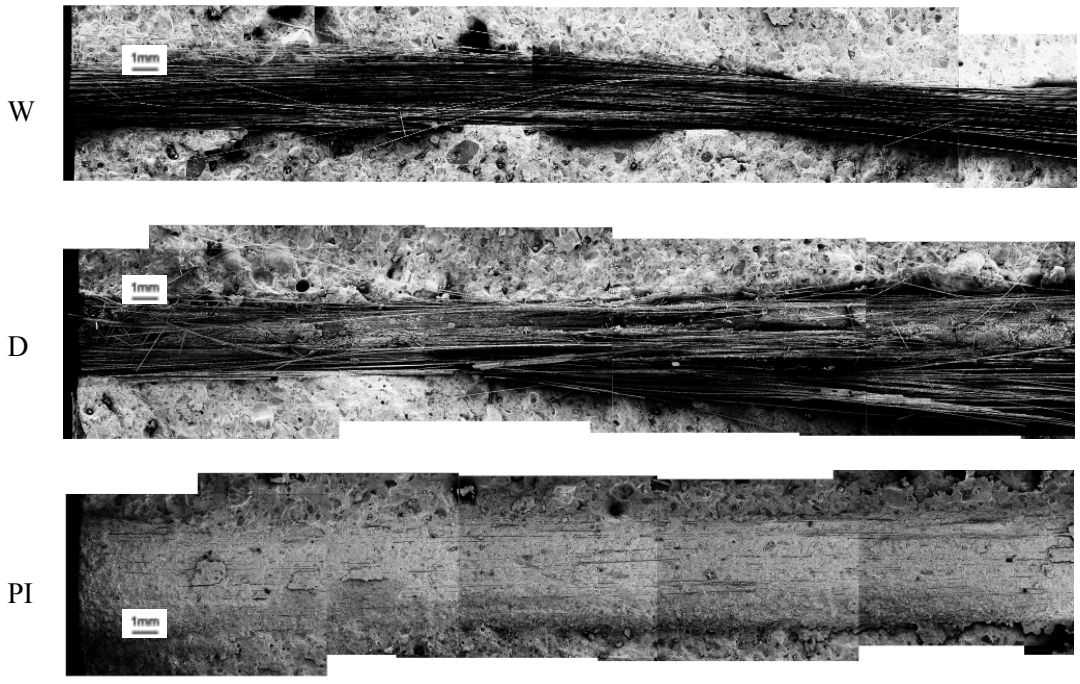

Fig. 2: OC2 yarn; longitudinal sections; W, D and PI pre-treatments.

The SEM observation allows the average penetration depth of the cementitious matrix into the yarn to be estimated. From this estimate, an impregnation index i_y was calculated as the ratio of the impregnated area to the apparent area of the cross-section of the yarn. It was determined considering a cylindrical shape of the yarn with constant penetration depth of the matrix, which are both strong assumptions regardless to the complexity of the shape of the impregnated yarn. Table 2 gives the values of the geometrical properties of the impregnated yarns, determined from the SEM observation.

As a consequence of the observed variation of the penetration of the cement paste inside the yarns, the values of the impregnation index varies significantly with the pre-treatment applied to the yarn. W pre-treatment, by water-saturating the porosity of the yarn, prevents the yarn from matrix penetration and gives the lowest values of the impregnation index. D pre-treatment leads to an important increase of the impregnation index for SG2, SG3 and OC1 yarns when the increase was almost unobserved for SG1 and OC2 yarns. PI pre-treatment, by forcing the penetration of the matrix inside the yarn, is supposed to allow the full impregnation of the yarn to be obtained (i_Y = 100 %).

It should be noticed that, due to the strong idealization made for the calculation and to the variability of the measurement of the penetration depth, the impregnation index should not be considered as a fine quantification of the impregnation but only as a qualitative estimate.

Table 2: Characteristics of the impregnated yarns.

Configuration	Diameter of the impregnated yarn [μm]	Observed penetration depth [μm]			i_Y
		Min.	Mean	Max.	
SG1 W	3190	100	125	150	15%
SG1 D	4270	300	325	350	28%
SG1 PI	3220				100%
SG2 W	2841	153	225	321	29%
SG2 D	3141	440	714	1002	70%
SG2 PI	3422				100%
SG3 W	2986	487	664	803	69%
SG3 D	2760	1380	1380	1380	100%
SG3 PI	3090				100%
OC1 W	3520	250	375	500	38%
OC1 D	3260	600	700	800	67%
OC1 PI	4190				100%
OC2 W	2690	160	170	180	24%
OC2 D	3390	160	170	180	19%
OC2 PI	4260				100%

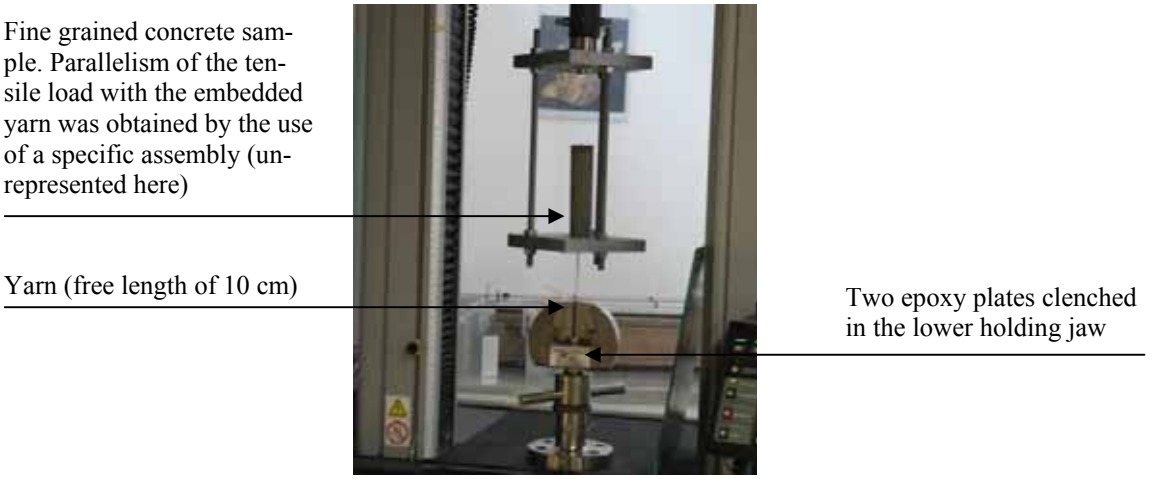

Fig. 3: Pull-out device.

3 Mechanical pull-out behaviour of the embedded yarns

3.1 Testing method

The load-displacement (P-δ) curves for the pull-out tests were obtained from tension test performed with a universal testing device (30 kN capability) as described in ALJEWIFI ET AL. [11]. The pull-out tests were made by applying a tensile load on the free end of a yarn. One side of the yarn was embedded in a fine grained concrete cylinder (the embedded length was chosen in the following series: 1, 3, 5, 10, 15 or 25 cm). The end of the other side was glued in between two epoxy plates that were clenched into the lower holding jaw of the testing device. The free length of the yarn was 10 cm. It was not reduced to zero to avoid shearing stresses in the yarn during the mechanical testing. Fig. 3 gives an overview of the experimental setup.

Loading was applied at constant strain rate (0.01 mm/min). At least three samples were tested for each yarn / pre-treatment / embedded length configuration.

Three different stages are usually observed for the pull-out behaviour of yarns (St1 to 3 in Fig. 4). The first stage (St1) corresponds to the progressive loading of the filaments. It is characterized by delayed activation of the filaments associated to the progressive failure of few of them when load is reaching ultimate value. In the second stage of the behaviour (St2), the ultimate load is reached and the anchored filaments progressively fail, leading to a progressive decrease of the load when the pull-out displacement is increased. The third stage (St3) of the pull-out behaviour corresponds to the residual friction of the intermixed broken filaments. It is characterized by a slowly decreasing level of load. This last stage was observed only for W or D pre-treated yarns.

3.2 Determination of the anchorage length

The evolution of the ultimate pull-out strength P_{max} for increasing embedded length is given in Fig. 5 (case of SG1 yarn). When the embedded length is small, the ultimate pull-out load is an increasing function of the embedded length. Over a given value of the embedded length (named L_{lim} in the following), failure is still obtained by pull-out but the ultimate load becomes almost independent of the embedded length. This length L_{lim} is the anchorage length of the yarn. It corresponds to the length needed to have the maximum of filaments (but not necessarily all the filaments) in contact with the matrix over the embedded length, considering the twisted shape of the yarn. For embedded length lower than L_{min}, the number of anchored filaments and therefore the ultimate pull-out strength increases when the embedded length increases. Over L_{min}, the pull-out strength remains constant as a change of the embedded length does not modify the anchoring conditions of the filaments. L_{min} is influenced by the yarn pre-treatment. In particular, PI pre-treatment gives very low L_{min} (under 1 cm).

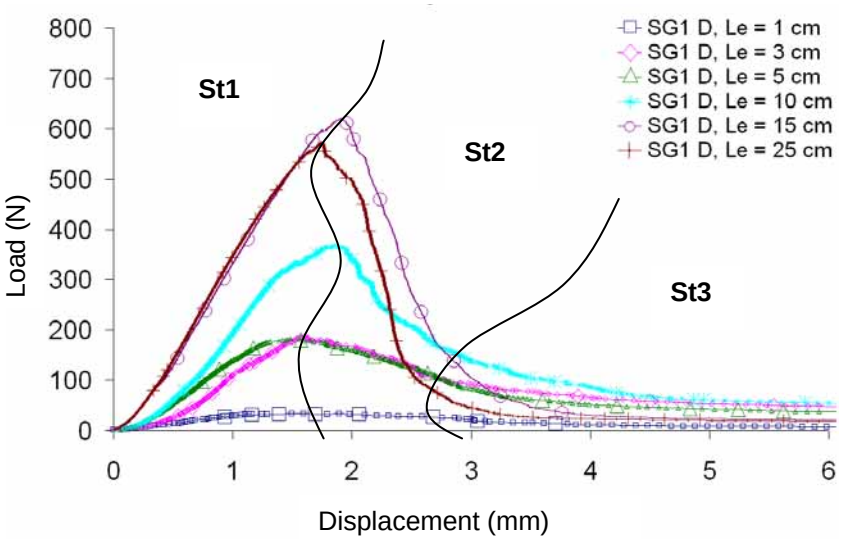

Fig. 4: Example of load-displacement curves; SG1 yarn, D pre-treatment; Le: embedded length.

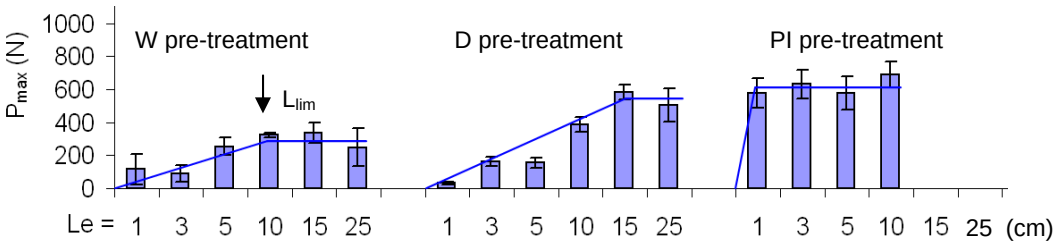

Fig. 5: values of the ultimate load P_{max} versus embedded length Le (example of SG1 yarn).

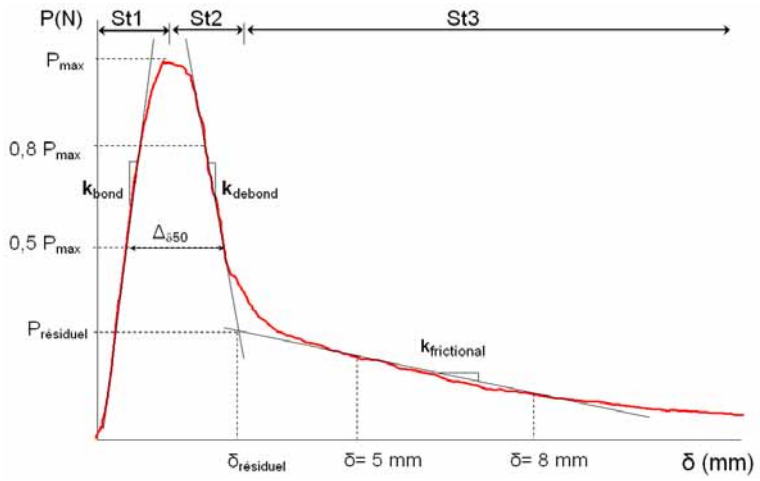

Fig. 6: Parameters of the pull-out behaviour to be derived from the force-displacement curve.

3.3 Pull-out behaviour of embedded yarns

Fig. 6 shows the parameters retained as characteristic for the pull-out behaviour of the embedded yarns: ultimate pull-out strength P_{max}; stiffnesses k_{bond} and k_{debond} of the first and second stages of the pull-out behaviour; stiffness $k_{frictional}$ of the third stage (residual load); and second to third stages transition load $P_{residual}$.

The stiffnesses are determined as the slope of the least square line corresponding to the measurements made in the dedicated range:
– 0.5-0.8 P_{max} in the first stage (pre-peak) part of the (P-δ) curve for k_{bond},
– 0.5-0.8 P_{max} in the second stage (post-peak) part of the (P-δ) curve for k_{debond},
– 5-8 mm displacement in the third stage (residual load) part of the (P-δ) curve for $k_{frictional}$.

As a result of the configuration of the test, it is important to note that these stiffnesses depend not only on the pull-out behaviour but also on the tensile behaviour of the free length of the yarn.

$P_{residual}$ is determined as the load given by the intersection of the second and third stages least square lines, with respect to the previous ranges.

We retain as characteristic of the pull-out behaviour of one yarn / pre-treatment configuration the average values of the behaviour parameters obtained for yarn / pre-treatment / embedded length configurations with embedded lengths over L_{lim}. In the followings, the corresponding values are written with the same notation as defined at the beginning of this part, with addition off the index “lim”.

Table 3 gives the values (mean value and relative standard deviation) obtained for the characteristic parameters of the pull-out behaviour for the five types of yarns and for the three pre-treatments which have been tested.

For all parameters, the highest values were obtained with PI pre-treatment. The lowest values were obtained with W pre-treatment, with the exception of SG3 and OC1 yarns for which the lowest values are obtained with D pre-treatment.

We notice that the relative standard deviation is much more important after the peak load has been reached than before. Due to the complexity of the yarn / matrix interaction, pull-out behaviour becomes less foreseeable as the number of broken filaments increases.

Table 3: Parameters characteristic of the pull-out behaviour.

		$P_{max,lim}$		$k_{bond,lim}$		$k_{debond,lim}$		$k_{frictional,lim}$		$P_{residual,lim}$	
		M.	RSD	M.	RSD	M.	RSD	M.	RSD	M.	RSD
		[N]	[%]	[N/mm]	[%]	[N/mm]	[%]	[N/mm]	[%]	[N]	[%]
SG1	W	303.2	21	240.5	18	203.1	37	2.7	80	43.6	50
	D	543.2	14	358.1	10	669.3	33	2.0	26	26.0	36
	PI	632.3	14	395.0	12	1451.0	59	-	-	-	-
SG2	W	423.6	27	255.8	33	474.6	75	2.7	59	39.2	60
	D	471.1	21	289.4	11	517.7	59	4.4	52	49.0	53
	PI	722.1	17	384.5	8	1747.0	55	-	-	-	-
SG3	W	565.1	13	344.2	7	755.0	43	2.6	50	43.5	64
	D	518.1	12	342.0	12	702.4	41	3.0	49	37.5	57
	PI	751.2	12	442.9	10	1431.8	19	-	-	-	-
OC1	W	319.7	17	329.7	26	478.1	72	2.1	75	34.0	89
	D	335.7	4	353.8	9	307.4	7	1.6	*	14.2	*
	PI	376.5	16	392.6	76	2704.2	0.3	-	-	-	-
OC2	W	203.1	15	233.8	20	341.8	48	1.4	25	39.6	23
	D	324.6	23	326.4	22	699.8	43	4.5	39	64.1	31
	PI	434.1	8	346.3	16	2165.4	41	-	-	-	-

M.: Mean value; RSD: relative standard deviation

(-): no detectable third stage on the (P-δ) curve.

(*): only one sample on three gave a detectable third stage.

4 Relationship between pull-out behaviour and yarn flow properties

4.1 Flow rate measurements

A yarn is a porous structure which porosity is strongly dependent on the geometry of the filaments and on their orientation. Because the yarns used in this study are all made with parallel or approximately parallel filaments, their porosity is strongly oriented and favours the fluid transfer along the axis of the yarn. Therefore, a flow test has been used to characterise the porosity of the yarn. As the penetration of cement paste inside the yarn fills at least par-

tially the inter-filament porosity, this test is a way of quantifying the impregnation state of the yarn.

The flow test used consisted in determining the stabilized flow rate of water along an embedded yarn, for an imposed pressure gradient of 1075 Pa/cm. Experiments were conducted at 20°C. The flow rate was determined from the record of the time evolution of the flown volume (periodical optical reading during the test; duration of the test: one week). Samples were 2 cm long portion of the cylindrical specimens described in section 2.2. Two measurements were made in all cases. The flow rate through the mortar body (determined from measurements made on reference mortar specimens casted without yarn) is deducted from the measured flow rate through the specimen, which allows the yarn water flow to be precisely calculated. As the diameter of the impregnated yarns varies depending on the type of yarn and pre-treatment used (see Table 2), the flow rate is determined for a 1 mm² cross section of the impregnated yarn. Fig. 7 gives the obtained values. Except in the case of SG1 yarn, PI pre-treatment prevents the water to flow through the yarn by ensuring a complete filling of the inter-filament voids with cement paste.

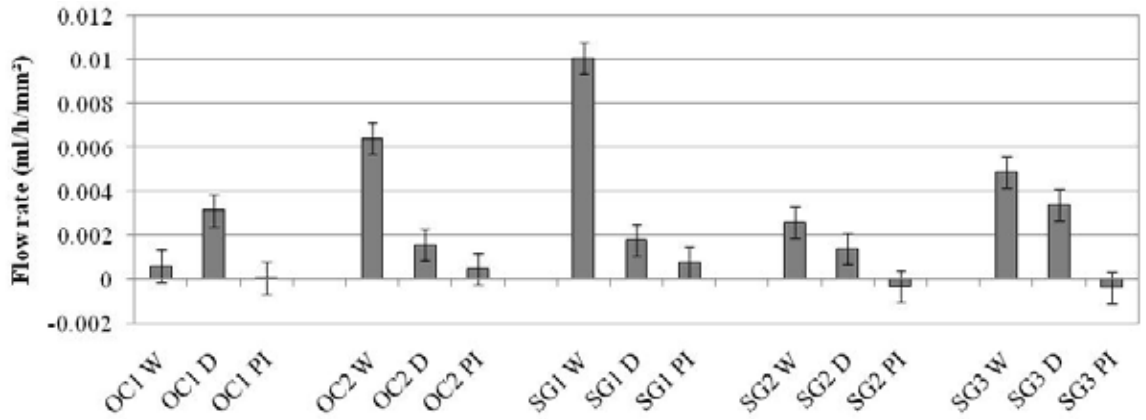

Fig. 7: flow rates measured for the tested configurations.

4.2 Relationship to the pre-peak pull-out behaviour

The pre-peak stage of the pull-out behaviour (stage 1 : St1 on Fig. 6) is characterized by the maximum pull-out load $P_{max,lim}$ and the first stage stiffness $k_{bond,lim}$. Fig. 8 and 9 give respectively the evolution of $P_{max,lim}$ and $k_{bond,lim}$ with the flow rate. As the penetration of the matrix in the yarn reduces the flow of water and increases the number of anchored filaments, an increase of the flow rate is associated to a decrease of the pull-out ultimate load $P_{max,lim}$ and stiffness $k_{bond,lim}$ (dash lines in Fig. 8 and 9 define the general trend). The correlation with the flow rate is particularly good in the case of k_{bond} where it seems to be almost uninfluenced by the type of the yarn. In the case of the pull-out ultimate load $P_{max,lim}$, SG yarns give highest

ultimate loads than OC yarns. This may be a consequence of the type of sizing used. SG yarns are manufactured for a used in concrete and their sizing should favour the yarn / concrete adhesion. OC yarns are designed for a use in polymer matrix and their sizing may be less compatible with concrete than in the case of SG yarns.

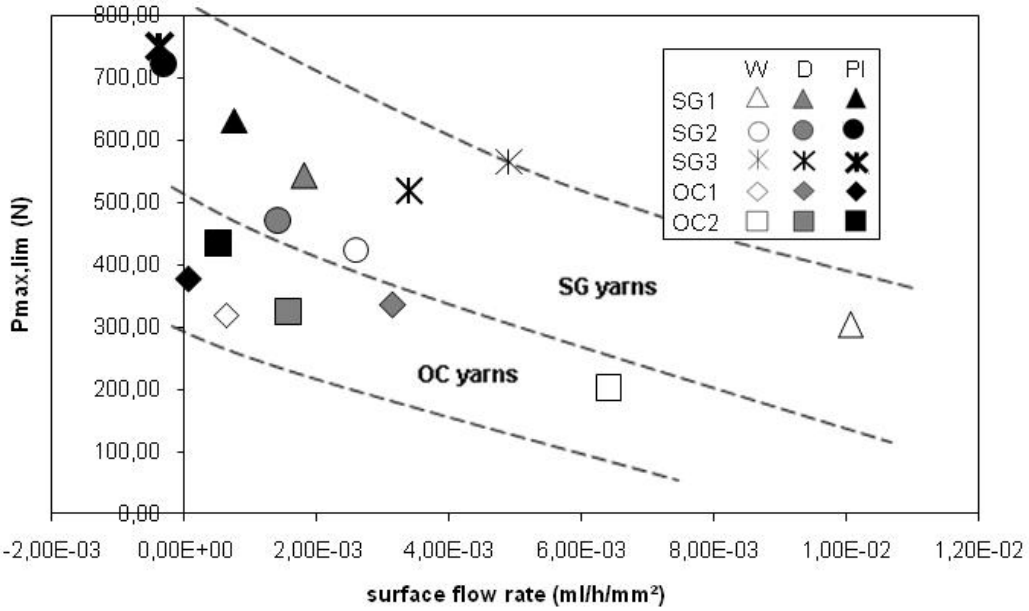

Fig. 8: $P_{max,lim}$ vs. flow rate.

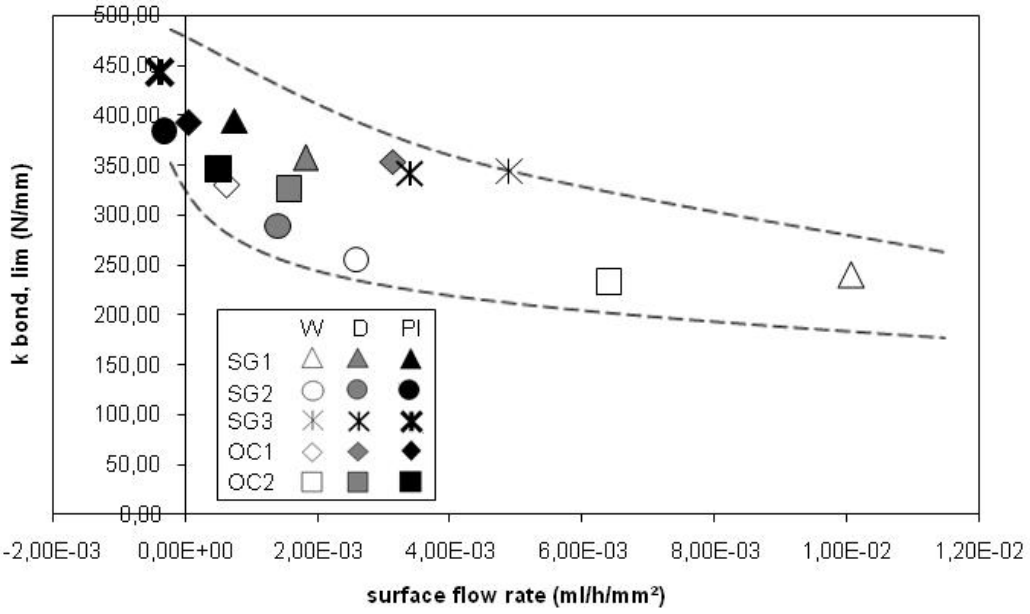

Fig. 9: $k_{bond,lim}$ vs. flow rate.

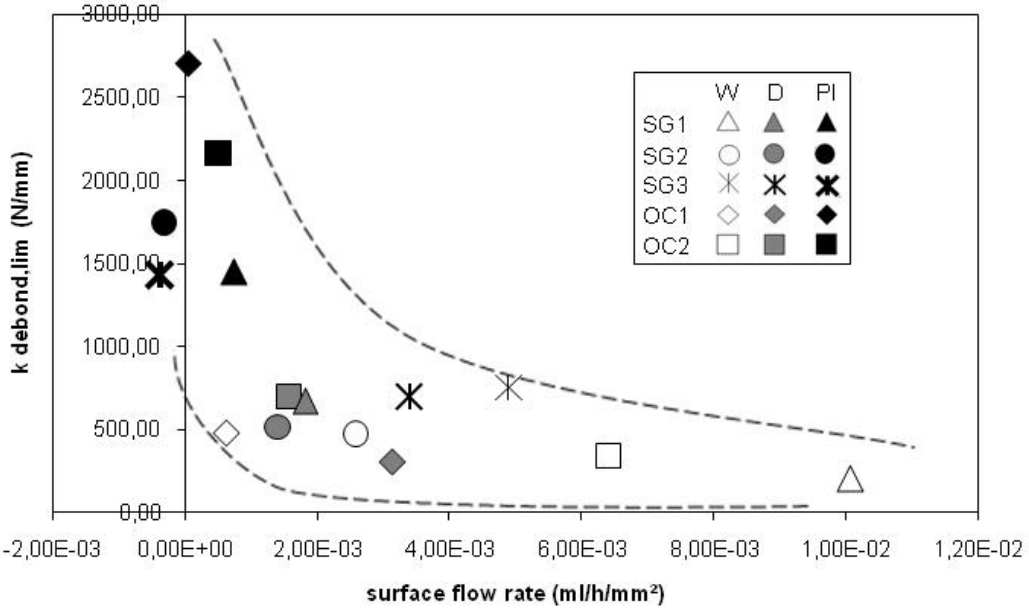

Fig. 10: $k_{debond,lim}$ vs. flow rate.

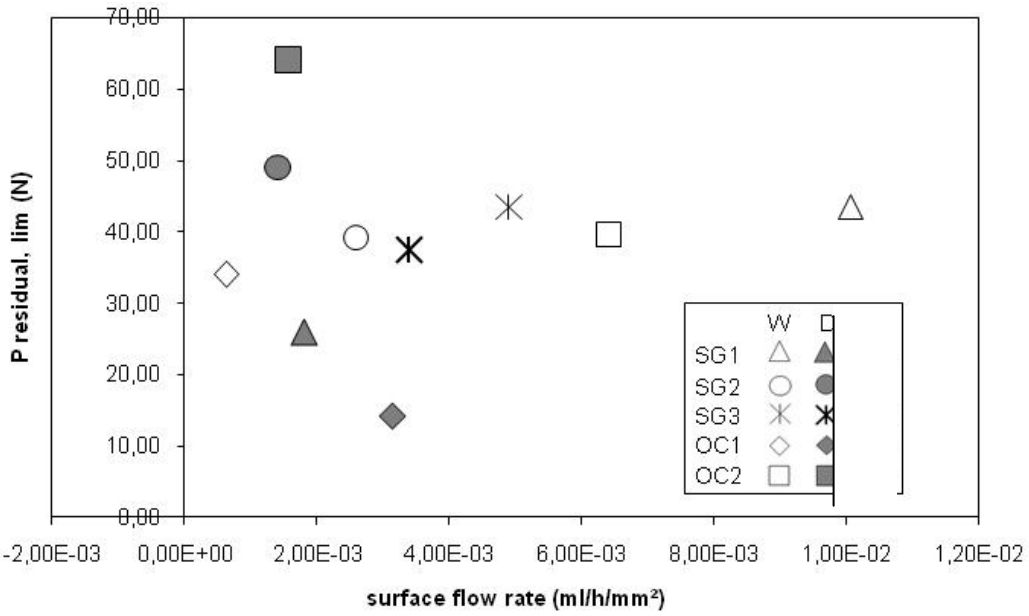

Fig. 11: $P_{residual,lim}$ vs. flow rate.

4.3 Relationship to the post-peak pull-out behaviour

The post-peak stage of the pull-out behaviour (stage 2: St2 on Fig. 6) is characterized by second stage stiffness $k_{debond,lim}$. Fig. 10 gives the values of $k_{debond,lim}$ versus the flow rate. The relationship to the flow rate is similar to those observed for $k_{bond,lim}$ (Fig. 9) with enhanced

variation of the stiffness. Whatever the type of the yarn is, values of $k_{debond,lim}$ are low for W and D pre-treatments, when they vary significantly with the type of yarn for PI pre-treatment.

4.4 Relationship to the residual pull-out behaviour

The residual pull-out behaviour (stage 3: St3 on Fig. 6) is characterised by the residual stiffness $k_{frictional,lim}$ and the remaining load $P_{residual,lim}$. It is observed only with W or D pre-treated yarns. The residual behaviour depends on the sequences of failures in the previous phases. As these sequences are specific to each embedded yarn, the resulting residual behaviour largely differs from one test to the other, which justifies the high standard deviations that are observed for the residual stage characteristic parameters. Results obtained for the residual behaviour should therefore be taken with caution.

Fig. 11 gives $P_{residual,lim}$ versus the flow rate. It can be shown that, in the case of W Pre-treated yarns, $P_{residual,lim}$ is not linked to the flow rate. In the case of D pre-treated yarns, $P_{residual,lim}$ seems to decrease sharply with increasing flow rates.

The same trends are observed for $k_{frictional,lim}$, as $k_{frictional,lim}$ and $P_{residual,lim}$ are almost linearly correlated.

5 Relationship between pull-out behaviour and yarn porosity

5.1 Yarn porosity measurements

As the penetration of cement paste inside the yarn should occupy a portion of the inter-filament voids, it appears that the measurement of the inter-filament porosity should be a way to quantify the impregnation of the yarn.

To evaluate the porosity which is specifically associated to the presence of a multifilament yarn (inter-filament porosity and matrix / yarn interface porosity), a specific method was developed based on mercury intrusion porosity measurements. It consists in a comparison of the pores distribution of the studied sample (a yarn embedded in a cementitious matrix cylinder) to the pores distribution of the corresponding matrix. As explained by ALJEWIFI ET AL. [10], the comparison is made in the 0.3 to 3 μm range of pores diameter, determined as the more sensitive to the presence of a yarn. Fig. 12 gives the values obtained for the different yarns and pre-treatments.

With the exception of SG3 and OC1, which yarn pore volumes appear as rather uninfluenced by the pre-treatment, the yarn pore volumes are all the more high than the penetration of the matrix in the yarn is important (see Table 2 the relationship between pre-treatments and cement paste penetration depths). This was attributed to the mechanical actions applied on the yarn during the casting of the samples (or during the PI pre-treatment), that tend to disorgan-

ise the arrangement of the filaments and induce the creation of new voids in the yarn, in association with the penetration of the cement paste. In the case of W pre-treatment, tension forces associated to the initial saturation of the yarn with water tend to agglomerate the filaments and stabilise the yarn structure during the casting, inducing the lowest values of the yarn pore volume.

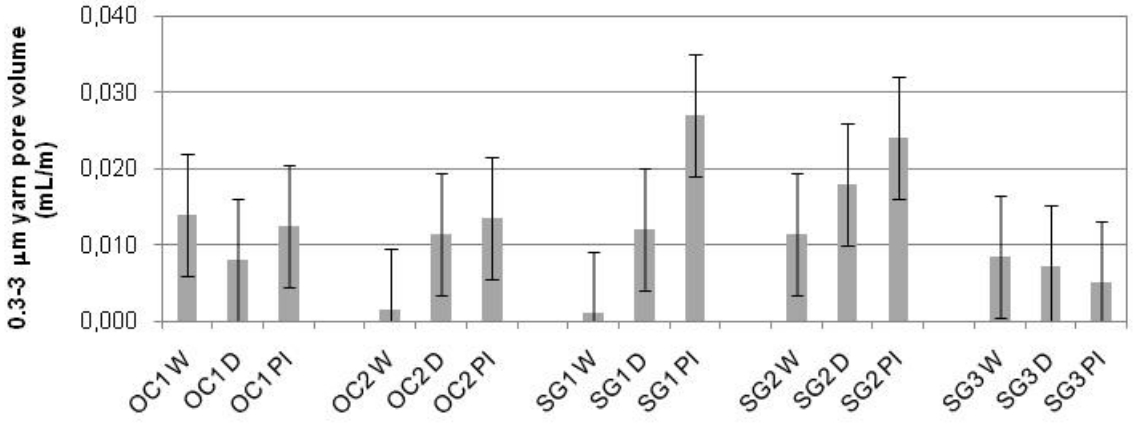

Fig. 12: 0.3-3 µm yarn pore volume (values are given for a yarn unit length of 1 m).

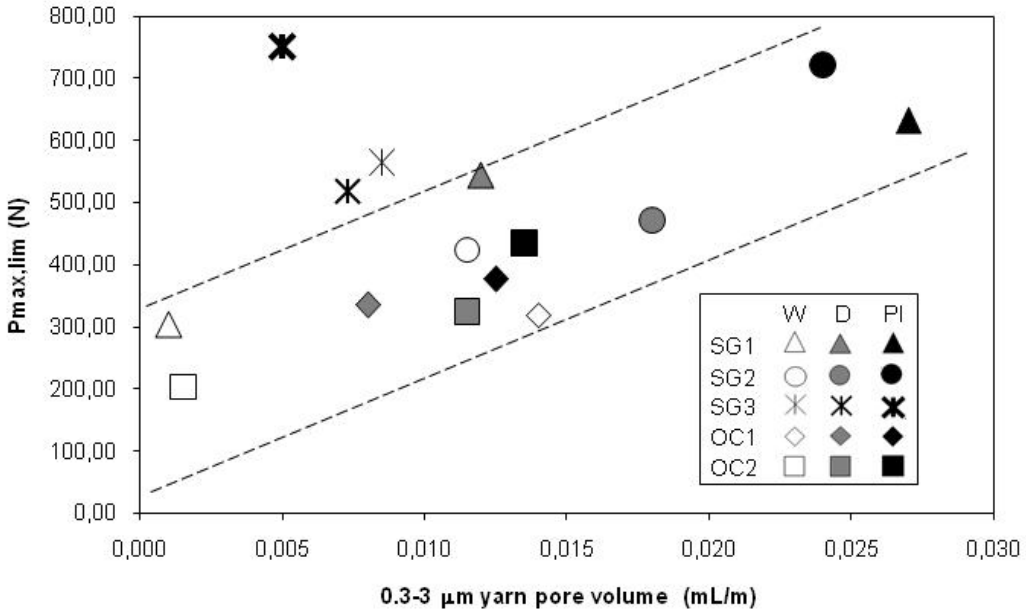

Fig. 13: $P_{max,lim}$ vs. yarn pore volume.

Fig. 15 gives the values of $k_{debond,lim}$ versus the yarn pore volume. This parameter is representative of the post-peak pull-out behaviour. As for $k_{bond,lim}$, $k_{debond,lim}$ increases when the yarn pore volume increases, with enhanced variation of the stiffness. In this case, if a general

trend is observed, it do not include the PI pre-treated yarns, contrary to what was observed for the relationship between post-peak stiffness and flow rates (Fig. 9).

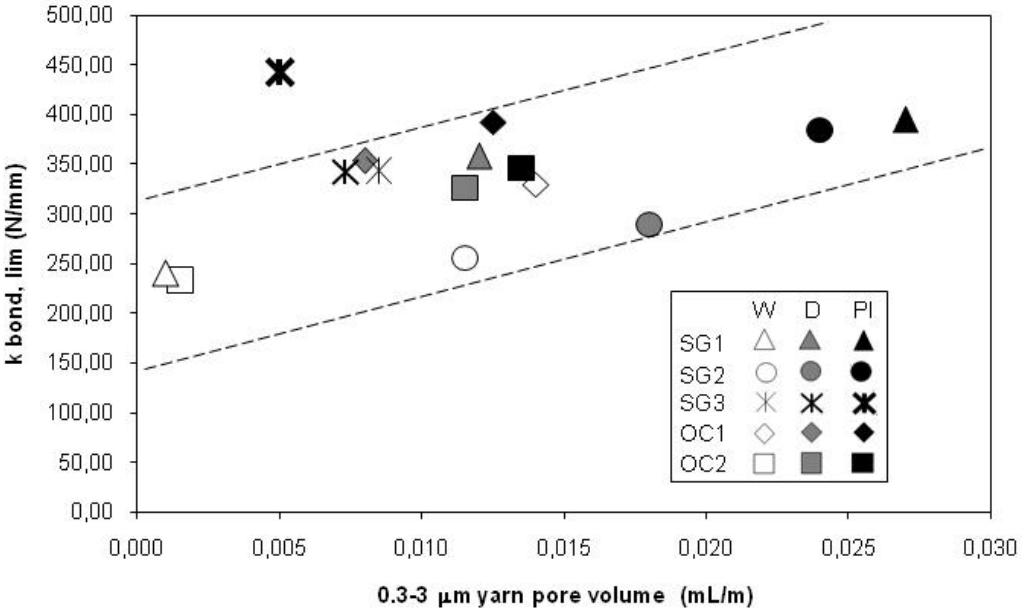

Fig. 14: $k_{bond,lim}$ vs. yarn pore volume.

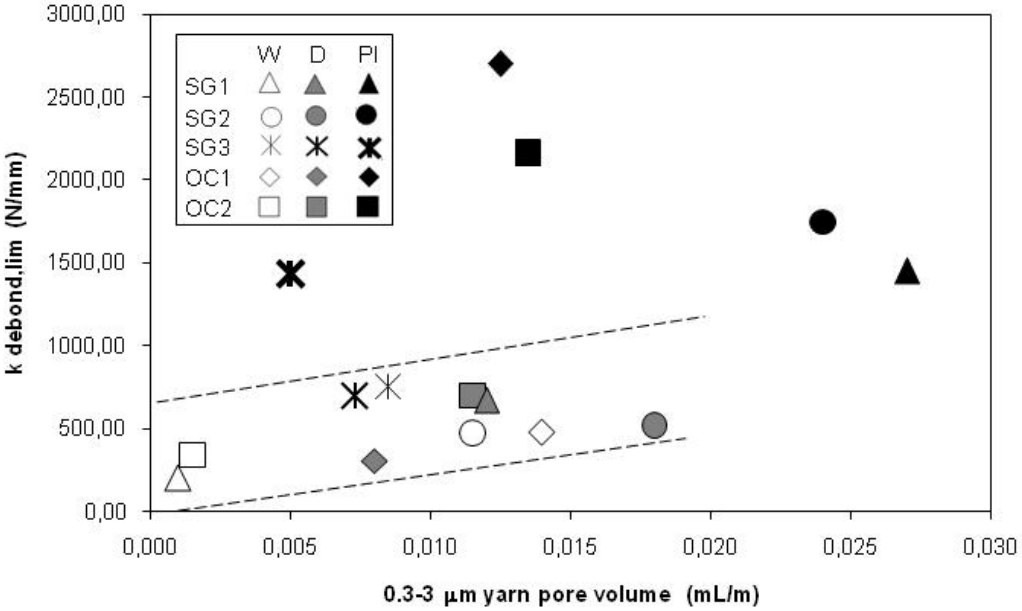

Fig. 15: $k_{debond,lim}$ vs. yarn pore volume.

The evolution of the residual load $P_{residual,lim}$, when the yarn pore volume changes (see Fig. 16), does not exhibit the general trend it does for the relationship with the flow rate. But,

with the care needed because of the lack of accuracy of the measurements made in the residual stage of the pull-out behaviour, all yarns (except SG1) give a higher value for $P_{residual,lim}$ when the yarn pore volume increases. The same observation is also made in the case of $k_{frictional,lim}$.

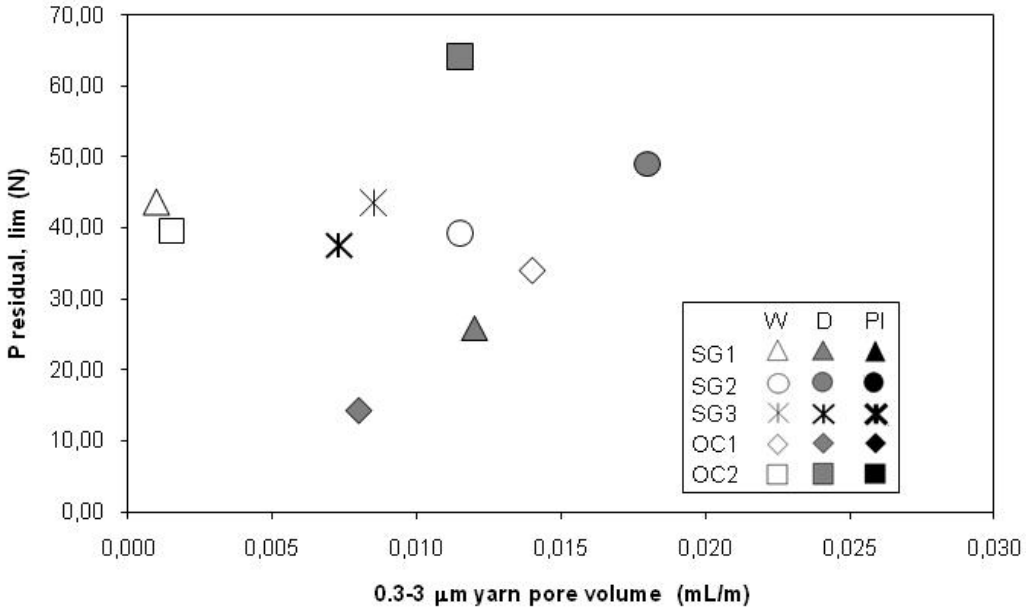

Fig. 16: $P_{residual,lim}$ vs. yarn pore volume.

6 Discussion

Sections 4 and 5 have shown that, under some conditions, parameters linked to the physical state of the impregnation of the yarn by the cement paste are directly connected to the mechanical properties of the pull-out behaviour. The relationships between the mechanical performances and the physical properties of the impregnation show sometimes a lake of accuracy, as they are characterised by relative standard deviations of the measurements that could be large (this is specially the case for the residual phase of the pull-out behaviour). Nevertheless, in most of the cases general trends can be drawn, but need more study to be defined with more accuracy.

Concerning the flow rate measurements, the results that have been presented suggest that this parameter can be used to make a global evaluation of:

– The penetration of the cement paste inside the yarn. The deeper the cement paste penetrates into the yarn, the lower the flow rate is. Consequently, a decrease of the flow rate should be associated to an increase of the ultimate load and of the pre- and post-peak stiffness (a deeper penetration increases the number of anchored filaments and therefore increases the load bearing for a given extraction displacement). These tendencies are clearly visible on Fig. 8, 9 and 10.

– The alignment of the filaments in the yarn, and particularly of the un-impregnated filaments. A yarn structure made, due to capillarity forces, of poorly impregnated parallel filaments should give high flow rates (well oriented parallel inter-filament pores favour the flow). This kind of structure should also induce an increase of the active length of the filaments (i.e. of the anchorage length of the filaments), which should induce a decrease of the stiffnesses, especially in the case of the post-peak behaviour (poorly impregnated parallel filaments should also favour the slip of the broken filaments). Fig. 9 and 10 show tendencies that are consistent with these mechanisms. In particular, the decrease of the post-peak stiffness $k_{debond,lim}$ when the flow rate increases is much more important than the decrease of the pre-peak stiffness $k_{bond,lim}$ in the same conditions (respectively rough reductions of 80% and 40%).

Concerning the yarn pore volume, the analysis which is made in section 5.1 has shown that this parameter could be a quantitative measurement of:

– The penetration of the cement paste inside the yarn. The same mechanism as previously described should make the ultimate load and the pre- and post-peak stiffnesses increase when the yarn pore volume (i.e. the impregnation) increases. This is what is experimentally observed (Fig. 13, 14 and 15).

– The disorganisation of the yarn structure. As explained in section 5.1, the increase of the yarn pore volume corresponds to the increase of the volume of pores of diameters in the range 0.3 to 3 μm, due to the disorganisation of the yarn structure induced by the pre-treatment and the casting. This disorganisation should also impact the alignment of the filaments and should generate more contacts between the filaments. The presence of cement paste should as well increase the number of contacts, as particles of cement paste could interact with filaments as a third body. Consequently, friction should increase when filaments slip (during the residual stage of the pull-out behaviour, but also during the post-peak behaviour), which was partially observed (Fig. 16). This phenomenon should also impact the stiffness, as an increased friction along the yarn will reduce the elongation of the yarn for a given pull-out load. This may explain why the PI pre-treated yarns give highest values for $k_{debond,lim}$, and sometime for $k_{bond,lim}$ than W or D pre-treated yarns.

7 Conclusion

Experimental investigations have been performed on 15 different associations of a multi-filament yarn embedded in a fine grained concrete matrix and a yarn pre-treatment. The results that have been obtained give information on the mechanical pull-out behaviour and on the physical state of the impregnation (flow rate and yarn pore volume). Analysis of the correlation between these two sets of parameters show that the physical parameters can be used as quantifiers of the impregnation state of the yarns and connected to the mechanical performances. The flow rate measurement appears as being particularly significant for the pre- and

post-peak pull-out behaviour, when the yarn pore volume appears as much more linked to the behaviour phases that involved friction (post-peak and residual phases).

The results previously presented are nevertheless complex to interpret, because the specific structure of impregnated yarns generates multi-influenced behaviour. In particular, the specific role of the sizing has been almost ignored in our study. In reality, the surface properties of the filaments may largely influence the penetration of the cement paste into the yarn and also the physical measurements themselves (and in particular the measurement of the flow rate). The impact of this factor must be studied to reach a more precise understanding of the phenomena that have been studied and described in this work.

8 References

[1] JESSE, F.; CURBACH, M.: The present and the future of the textile reinforced concrete. In: BURGOYNE, C. (EDS.) *HRPRCS5 fiber-reinforced plastics for reinforced concrete structures, July16-18, 2001, Cambridge*, *UK*, pp. 593–605

[2] BRAMESHUBER, W.; BROCKMANN, T.; BANHOLZER, B.: Textile reinforced ultra high performance concrete. In proceedings: *International Symposium on UHPC, September 13-15, 2004, Kassel, Germany*., pp. 511–532

[3] HEGGER, J.; ZELL, M.; HORSTMANN, M.: Textile Reinforced Concrete – Realization in applications. In proceedings: *International fib Symposium Tailor Made Concrete Structures: New Solutions For Our Society, May 19-22, 2008*, *Amsterdam, Netherlands,* pp. 357–362.

[4] HANISCH, V.; KOLKMANN, A.; ROYE, A.; GRIES, T. Yarn and textile structures for concrete reinforcements. In proceedings: *International Symposium and Workshop on Ferrocement and Thin Reinforced Cement Composite, FERRO-8, February 6-8, 2006, Bangkok, Thailand.*

[5] KONRAD, M.; CHUDOBA, R.; BUTENWEG, C.; BRUCKERMANN, O.: Textile reinforced concrete part II: Multi-level modeling concept. In proceedings: *International Kolloquium über Anwendungen der Informatik und der Mathematik in Architektur und Bauwesen, Jun10-12, WEIMAR , BAUHAUS-UNIVERSITÄT, GERMANY.*

[6] PELED, A.; SUEKI, S.; MOBASHER, B.: Bonding in fabric-cement systems: effects of fabrication methods. *Cement and Concrete Research* 36 (2006), pp. 1661–1671

[7] OHNO, S.; HANNANT, D.J.: Modelling the stress-strain response of continuous fiber reinforced cement composites. *ACI Materials Journal* 91 (1994), pp. 306-312

[8] LANGLOIS V.: *Etude du comportement mécanique des matériaux cimentaires à renforts synthétiques longs ou continus.* Université de Cergy-Pontoise, France, 2004 - Ph.D

[9] HÄUßLER-COMBE, U.; HARTIG, J.: Bond and failure mechanisms of textile reinforced concrete (TRC) under uniaxial tensile loading. *Cement & Concrete Composites* 29 (2007), pp. 279–289

[10] ALJEWIFI, H.; FIORIO, B.; GALLIAS, J-L.: Characterization of the impregnation by a cementitious matrix of five glass multi-filament yarns. *European Journal of Environmental and Civil Engineering* 14 (2010), pp. 529–544

[11] ALJEWIFI, H.; FIORIO, B.; GALLIAS, J-L.: Pull-out behaviour of a glass multi-filaments yarn embedded in a cementitious matrix. In proceedings: *EURO-C 2010, March 15-18, 2010, Rohemoos/Schladming, Austria*, pp.77-86